Carbon-nanotube junctions

Controlled Carbon-Nanotube Junctions Self-Assembled from Graphene Nanoribbons**

*Lan He, Jun-Qiang Lu, and Hanqing Jiang**

Although considerable progress has taken place in the area of carbon nanotube (CNT) junction synthesis,[1–3] properties,[4,5] and applications,[6–8] major obstacles still remain in controlled synthesis, posing significant limitations for the development of new CNT-based applications. Existing approaches for synthesizing CNT junctions do not produce CNT junctions with good controllability or favorable selectivity and yield. Here, we report a new approach for synthesizing CNT junctions based on a self-assembling process from two tailored graphene nanoribbons (GNRs). CNT junctions with two, three, and four terminals, starting from GNRs either with perfect or irregular tailoring, are synthesized. The functionality of these self-assembled CNT junctions for nanoelectronics is then confirmed using charge-transport simulations. Based on state-of-the-art experimental capability, this approach with identified scalability down to the atomic scale and screening-free selectivity is practically realizable and desirable for individually controlling both the chirality and shape of CNT junctions, thereby dramatically improving their effectiveness and further expanding their application repertoire.

Existing approaches for synthesizing CNT junctions primarily inherit from that of CNTs and intrinsically bear some shortcomings. As a result, the scientific community desires a new approach capable of precisely controlling the synthesis of CNT junctions. Geometrically, the synthesis of CNTs can be ''imagined'' as a rolling process of a narrow graphene ribbon. The appearance and manipulation of GNRs[9–12] make the imaginary ''rolling-up'' process promising. The literature thus far has demonstrated the ability to realize single or multilayers of freestanding GNRs with well-defined nanoscale width (as narrow as 2.5 nm) and lattice-defined graphene edges (armchair versus zigzag).[13–15] Furthermore, theoretical studies on GNRs[16–18] have suggested that GNR edges (especially zigzag edges) have good chemical reactivity due to their unique electronic state near the Fermi level that is localized at the edge carbon atoms. This reactivity leads to the spontaneous emergence (i.e., a self-assembly process) of planar reconstruction for zigzag edges, achievable even at room temperature. It is expected that active GNR edges will play a crucial role in the self-assembly of tubular structure and CNT junctions from patterned GNRs. A series of these self-assembly processes are conducted based on the pretailored GNRs.

The self-assembly process begins with two identical layers of GNRs at the natural separation (i.e., 0.34-nm spacing) shown in Figure 1a, which corresponds to two freely suspended GNRs in a vacuum, having been realized in experiments.[10] By controlling the edge type and width of GNRs, the formed CNTs can achieve specific chirality. Insets of Figure 1a illustrate one zigzag GNR with width $N_z = 5$ that can form a (5, 5) armchair CNT and one armchair GNR with width $N_a = 10$ that can form a (10, 0) zigzag CNT (see Supporting Information S1). This step is experimentally feasible due to current GNR patterning technology that is able to tailor two bent junctions (zigzag/armchair/zigzag or armchair/zigzag/armchair).[13,14] A canonical ensemble (NVT) of molecular dynamics (MD) simulation is used to simulate the system of two patterned GNRs with 1 412 atoms. Figure 1b shows a seamless (5, 5)–(10, 0)–(5, 5) CNT junction self-assembled from two GNRs (Figure 1a).

In addition to starting with two freely suspended GNRs in a vacuum, this self-assembly process can also occur with two GNRs supported by various substrates (e.g., highly oriented pyrolytic graphite (HOPG) or Si/SiO_2). To possibly align with future experiments on CNT junction synthesis, we use two GNRs lying on a very large graphite substrate (Figure 1c). Compared with Figure 1b for freely suspended GNRs, almost identical CNT junctions are formed from two GNRs supported by a graphite substrate (Figure 1d). This suggests that the substrate does not impose significant constraints on the self-assembly process due to the absence of activated atoms over the region where the substrate interacts strongly with GNRs. Consequently, the same conclusion is also valid for other substrates, thus substantially broadening the applications of this self-assembly method, specifically for the direct fabrication of CNT-based nanoelectronics.

The self-assembly process is the result of searching the minimum energy pathway for two layers of zigzag/armchair/zigzag GNRs (Figure 1a) where the total energy increases

[*] Prof. H. Jiang, Dr. L. He
School of Mechanical, Aerospace, Chemical and Material Engineering
Arizona State University
Tempe, AZ 85287 (USA)
E-mail: hanqing.jiang@asu.edu
Prof. J.-Q. Lu
Department of Physics and Institute for Functional Nanomaterials
University of Puerto Rico
Mayaguez, PR 00681 (USA)

[**] J.Q.L. acknowledges the start-up support from the University of Puerto Rico. H.J. is grateful for financial support from NSF CMMI- 0844737. The School of Mechanical, Aerospace, Chemical, and Material Engineering of Arizone State University is acknowledged for financial support of the colour images in this Communication.

Supporting Information is available on the WWW under http://www.small-journal.com or from the author.

DOI: 10.1002/smll.200900911

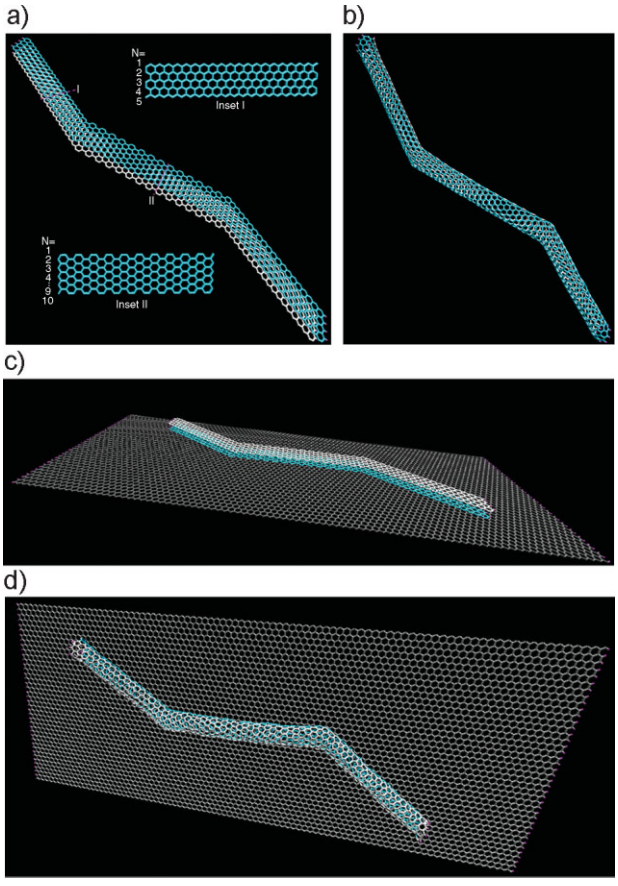

Figure 1. Formation of CNT junctions from two GNRs. a) The initial configuration of two identical layers of zigzag/armchair/zigzag Z-shaped GNRs separated by the distance of 0.34 nm. The length for zigzag/armchair/zigzag GNRs are 20, 30, and 20 hexagonal rings, respectively. Two colors (cyan and white) denote two graphene layers with a total of 1 396 carbon atoms and the magenta at the right/left ends represents hydrogen bonds (16 hydrogen atoms). Inset I: the geometry structure of zigzag GNR. The width of zigzag GNR N_z is the number of zigzag chains across the width direction. Inset II: the geometry structure of armchair GNR. The width of armchair GNR N_a is the number of dimer lines across the width direction. b) The snapshot ($t = 4$ ns) of the Z-shaped CNT junction formed by the self-assembly process of two Z-shaped GNRs (Figure 1a) at 3 000 K followed by the annealing simulation to 300 K. c) Two identical zigzag-armchair-zigzag GNRs lying on a graphite substrate. Blue and white denote GNRs; gray is the graphite substrate. The interlayer spacing between them is 0.34 nm. The total number of atoms is 8 692 (1 396 atoms in the two GNRs, 7 200 atoms in the graphite substrate, 96 hydrogen atoms). d) A snapshot ($t = 170$ ps) for a self-assembled Z-shaped CNT junction on a graphite substrate at $T = 3\,000$ K.

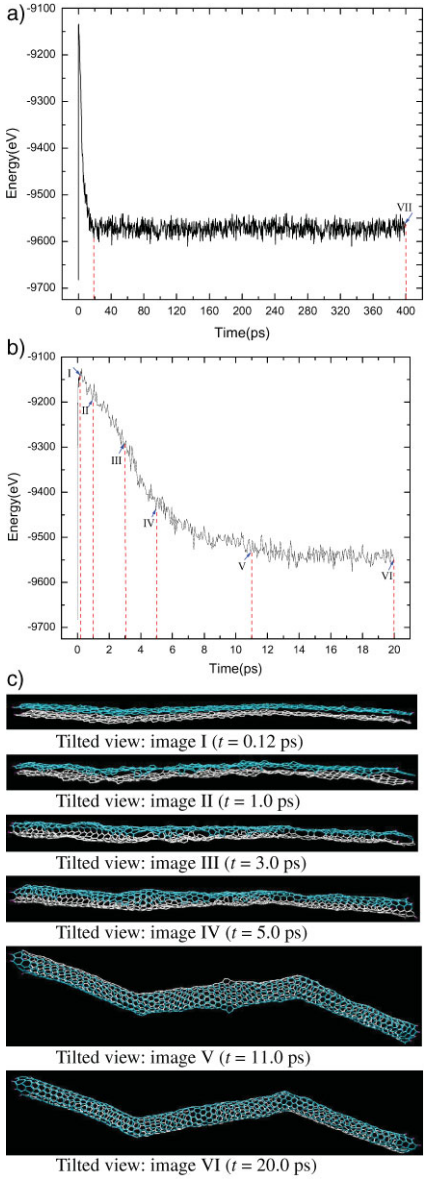

Figure 2. Calculated energy profile indicating the process of self-assembly. a) The energy profile as a function of time for the formation of a Z-shaped CNT junction self-assembled from two Z-shaped GNRs given by Figure 1a at $T = 3\,000$ K. b) A detailed energy profile for time period from 0 to 20 ps. Seven images demonstrate representative configurations during the process of self-assembly. In image I ($t = 0.12$ ps), thermal vibration of carbon atoms in two layers of GNRs increases system energy and leads to localized deformations (e.g., small ripples) instead of formation of new atomic bonds between two layers. At 1 ps (image II), a few new C–C bonds start forming from dangling bonds along zigzag and armchair edges driven by the van der Waals interactions between two layers, which leads to a decrease of the system energy. As time evolves (3.0 ps for image III and 5.0 ps for image IV), more new C–C bonds have been formed, which causes large curvature in each GNR and a continuous decrease of system energy. At 11 ps (image V), zigzag GNRs have formed a tubular structure while armchair GNRs still have unconnected dangling bonds between two layers, which confirms that zigzag edges have a more strongly localized electronic state across the Fermi level, making it easier for them to form tubular structures compared with the armchair edges.[16,17] At about $t = 20$ ps (image VI), the armchair GNRs also form the tubular structure and thus a seamless (5, 5)–(10, 0)–(5, 5) CNT junction has been self-assembled from zigzag/armchair/zigzag GNRs. Up to 400 ps (image VII), it is shown that the CNT junctions self-assembled from GNRs have been retained and the corresponding total energy is stable.

dramatically in the time range of $0 \approx 0.14$ ps, and then decreases with time, and finally reaches a relatively stable status with small fluctuations (Figure 2a). The process of self-assembly is clearly visible in the movies (see Supporting Information S2). The energy profile from 0 to 20 ps featured with a steep increase and decrease is detailed in Figure 2b, where six snapshots illustrate representative steps of bond formation between two layers of GNRs. These snapshots and the movies indicate three general steps of the self-assembly process: 1) localized deformation (e.g., ripples) where the energy dramatically increases (image I); 2) new bond formation due to chemical

reactions at the activated GNR edges, leading to energy decrease (images II–V); and 3) formation of a tubular structure with relatively minimal system energy (images VI and VII).

This self-assembly process is strongly temperature-dependent, the reason being that the temperature (e.g., 3 000 K for Figure 2) is what provides sufficient kinetic energy to overcome the reactivated barrier for forming CNT junctions from GNRs. Detailed discussion of the effect of temperature is given in Supporting Information S3. The stability of the self-assembled CNT junctions at high temperatures is studied by annealing simulations. It is found that the self-assembled CNT junction is stable at room temperature with the preserved identical configuration (including defects) (Figure 1b). Remarkably, the annealed Z-shaped CNT junctions self-assembled from GNRs have few defects (e.g., heptagons and pentagons) at the armchair/zigzag interfaces (see Supporting Information S4) and all carbon atoms are sp^2 hybridized.

One of the most commonly proposed applications of CNT junctions is supplanting silicon by providing basic building blocks for nanoelectronics. For example, the Z-shaped CNT junction (Figure 1b) is an ideal nanoscale field-effect transistor (FET). The armchair (5, 5) CNTs at the two ends naturally function as metallic electrodes and serve as the drain and source when a voltage V_{ds} is applied. The middle zigzag (10, 0) CNT acts as a semiconductor, which can then be turned to be conducting when applied a gate voltage V_g. Different from the existing CNT-FETs that use metals as electrodes,[19–21] the FETs proposed here based on CNT junctions replacing the metal electrodes with metallic CNTs. Thus in the Z-shaped CNT-FETs, the middle semiconducting CNT and the two metallic CNT electrodes that are well-connected via chemical bonds have excellent contacts, which effectively overcomes the problem of high-contact resistance in existing CNT-FETs as a result of the poor contacts between CNTs and metal electrodes.[19–21] It is expected that the Z-shaped CNT-FET will have better performance than existing CNT-FETs. Figure 3 presents the simulated charge-transport characteristics of the Z-shaped CNT-FET. Here, it is evident that the Z-shaped CNT-FET has a much larger drain–source current I_{ds} (i.e., ≈20 μA in Figure 3a) than existing CNT-FETs (i.e., only ≈2.0 μA in Figure 4a and ≈3.0 μA in Figure 5b in Reference [19]), even at a smaller drain–source V_{ds} (i.e., ≈0.5 V in Figure 3a versus ≈1.5 V in Figure 4a and Figure 5b[19]). Figure 3b shows that the Z-shaped CNT-FET will be turned from OFF to ON when the gate voltage reaches about 0.3 V. The ON/OFF current ratio (I_{ON}/I_{OFF}) is around 10^3 and can be further improved simply by increasing the length of the middle semiconductor CNT since the tunneling current I_{OFF} can be reduced exponentially with the length increasing.[22]

The versatility of the CNT junctions can be realized by various combinations of metallic and semiconducting terminals, which endows them with many fascinating applications for nanodevices.[23–26] The number, type, and geometry of multi-terminal junctions can be well-controlled by the self-assembly method starting from the two precisely pre-tailored GNRs. As a basic demonstration, three-terminal T-shaped and four-terminal cross-shaped CNT junctions can be formed from two pre-tailored T-shaped and cross-shaped GNRs (Figures 4a and c), respectively. The formed CNT junctions at $T = 3\,000$ K,

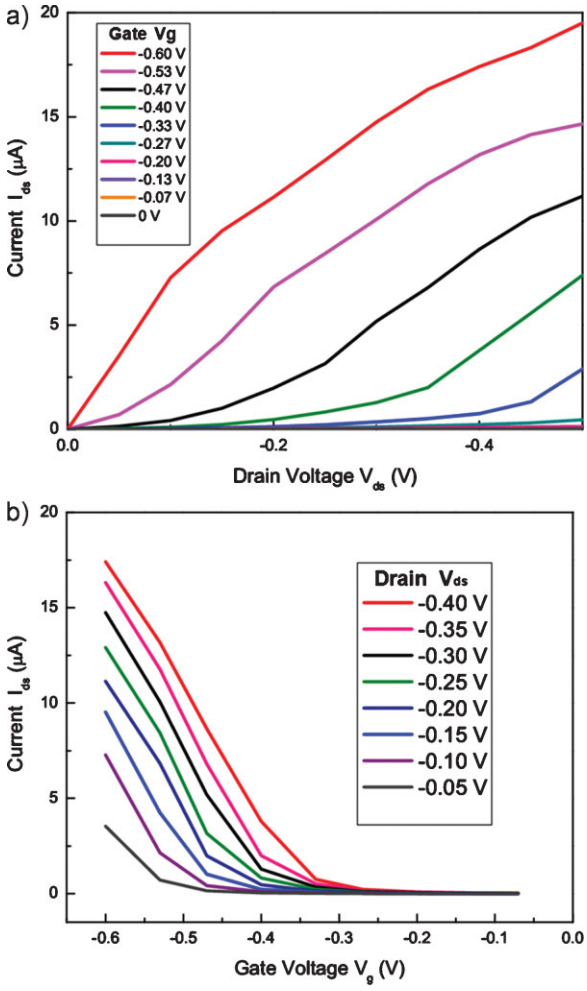

Figure 3. Charge-transport characteristics of a Z-shaped CNT-FET. a) I_{ds} of the Z-shaped CNT-FET as a function of V_{ds}. From bottom to top, V_g increases in steps of 0.067 V. b) I_{ds} as a function of V_g. From bottom to top, V_{ds} increases in steps of 0.05 V.

shown in Figures 4b and d, have few defects except one enneagon (highlight) at the crossing area. It is apparent that the formed T-shaped and cross-shaped CNT junctions can be utilized as triode or logic gates/switches.

Another advantage of this self-assembly approach, in addition to above-mentioned ability to control the chirality and type, is its robustness. In fact, this robustness ensures that this self-assembly approach is able to reproduce the experiments in which irregular (or rough) edges appear statistically during GNR tailoring. We here introduce some random roughness into the GNRs with perfect edges, characterized by a roughness probability $p \subset [0, 1]$ (see Experimental Section). To demonstrate the robustness of this approach, we choose a high roughness probability p for T-shaped GNRs (armchair-edged branch $p = 0.82$, and zigzag-edged stem $p = 0.76$) (Figure 5a). Figure 5b shows that GNRs with rough edges can still self-assemble a tubular T-shaped junction but with variable diameters and some defects, such as dangling bonds, polygons, and vacancies at the interjoints between two identical, but rough GNRs. The robustness ensures that this approach

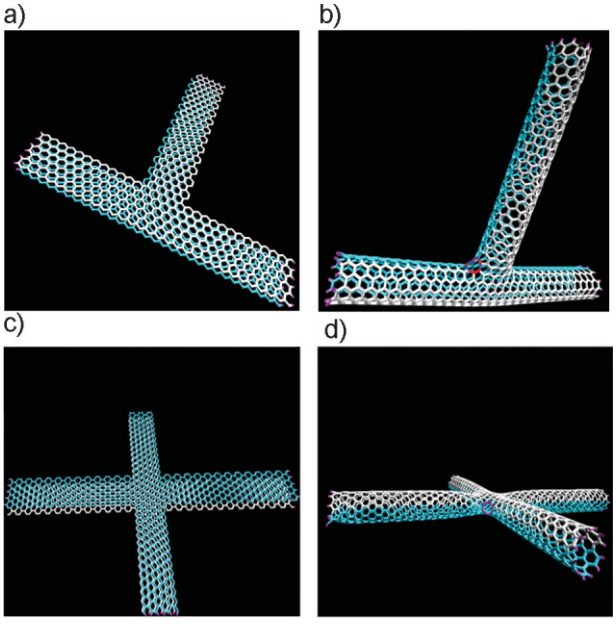

Figure 4. Formation of multi-terminal junctions. a) Two identical T-shaped GNRs ((6, 6) stem and (10, 0) branch) with total of 1 220 carbon atoms and 34 hydrogen atoms. b) A snapshot ($t = 400$ ps) for a self-assembled T-shaped CNT junction from T-shaped GNRs (Figure 4a) at $T = 3\,000$ K. One enneagon is highlighted using red and blue colors. c) Two identical cross-shaped GNRs ((6, 6) zigzag branches and (10, 0) armchair branches) with a total of 1 720 carbon atoms and 44 hydrogen atoms. d) A snapshot ($t = 400$ ps) for a self-assembled cross-shaped CNT junction from cross-shaped GNRs (Figure 4c) at $T = 3\,000$ K. One enneagon is highlighted using red and blue colors.

survives under extreme conditions and therefore has wide applications where the details (e.g., defects) are not vital, such as on nanocomposites.

This self-assembly method and the experiment technology enumerated here are mutually excited. The current experiment capabilities support the realization of this self-assembly method. The tailoring of GNRs with nanoscale precision in a vacuum has been successfully achieved[13–15] and provided pristine GNRs with activated edges, which validates the foundation of our approach. The GNRs used in previous simulations are about 1-nm-wide, however, wider GNRs can still self-assemble to CNTs junctions (see Supporting Information S5). This approach is robust enough to bear some degree of experimental uncertainty, such as irregular edges (as discussed previously). On the other hand, the theoretical understandings initiate a potentially promising direction for experiment development.

In summary, a controllable self-assembly approach of CNT junctions from GNRs has been developed. Two- and multi-terminal CNT junctions with various metallic and semiconducting branches have been formed. The experimental realization of this approach has been demonstrated by the formation of CNT junctions from GNRs with randomly rough edges. Such an approach provides an effective means for individually controlled synthesis of CNT junctions self-assembled from tailored GNRs and potentially broadens the applications of CNT junctions. The interplay of the ''unzipping'' approach (from CNTs to GNRs)[27,28] and the current self-assembly method (from GNRs to CNTs) will more intimately bridge these two carbon-based nanomaterials with versatile applications.

Experimental Section

Molecular dynamics simulations: All simulations are conducted in the constant temperature ensemble (NVT) where Langevin thermostats are used.[29] In the simulation system subject to the free boundary condition, the edge carbon atoms along the width direction are saturated by hydrogen atoms while dangling bonds still exist at the length edges. The interactions between C–C, C–H, and H–H atoms are characterized by the second-generation reactive empirical bond-order potential with 6–12 Lennard–Jones correction at long distance.[30] The predictor-corrector algorithm[29] is used to solve the equations of motion and a time step of 0.5 fs is used in all simulations. The energy minimization scheme is applied to the initial system and then the MD simulations of 800 000 time-step runs are carried out to relax the system and collect the data. The annealing simulations start from the formed Z-shaped CNT junction at 3 000 K and a 300 K temperature decrement is applied after each 800 000 MD equilibrium run.

Charge transport calculations: Using the atomic structures from the molecular dynamics simulations, the charge transport characteristics of the CNT junctions are calculated using a tight-binding model with one p orbital per carbon atom along with Green's function method.[31] Within the frame work of the Landauer approach, the CNT junctions are divided into three parts: one center part as the main functional device that is connected with two electrode parts from its left and right. The electron transmission function can be expressed as $T = \mathrm{Tr}(\Gamma_L G_C \Gamma_R G_C^+)$, where G_C is the Green's function of the conductor and Γ_L and Γ_R are the spectral densities describing the coupling between the electrodes and the device. The current can be obtained from integration of the transmission function.

$$I = \frac{2e}{h}\int_{-\infty}^{\infty} dE T(E, V_{ds}, V_g)[f(E-\mu_L) - f(E-\mu_R)] \quad (1)$$

with the electrochemical potentials in two electrodes $\mu_L = E_F - eV/2$ and $\mu_R = E_F + eV/2$.

Generation of rough edges: The roughness is characterized by two parameters: one to describe the number of atoms along the length direction deviated from the perfect edges, and the other to define the ratio of width variation to the width of a perfect GNR. The first parameter is given by the value of p ($0 \le p \le 1$), where p is the number of randomly picked edge atoms/number of total atoms in a perfect edge. The other parameter in this simulation is fixed to 20%. Thus, for a prescribed p value starting from the perfect edges, generation of roughness in the length direction is associated with adding or removing atoms at randomly picked positions of the edges. Edge geometries with the same p are totally different owing to the random generation.

Keywords:
carbon nanotubes · graphene · molecular dynamics simulations · nanoribbons · self-assembly

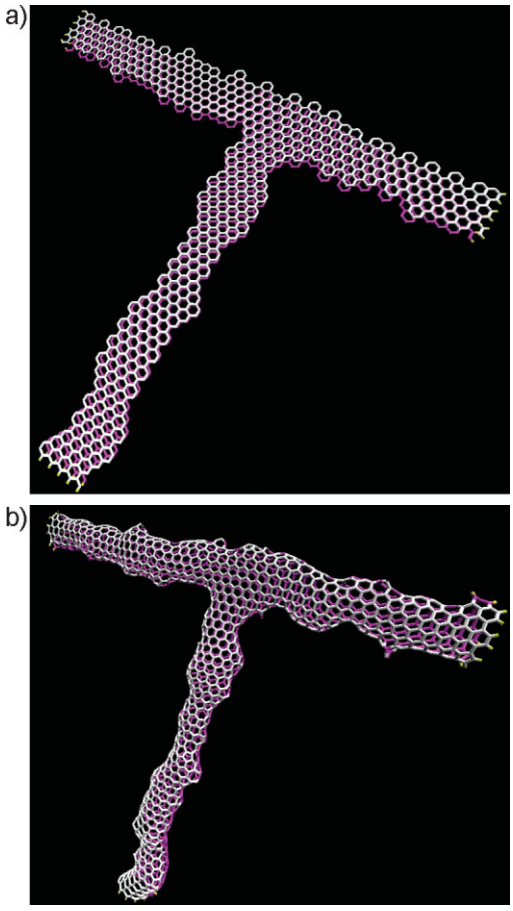

Figure 5. Effect of edge roughness on the formation of CNT junctions. a) Two identical T-shaped GNRs with rough zigzag ($p = 0.76$)/armchair ($p = 0.82$) edges include a total of 1 912 carbon atoms and 34 hydrogen atoms. Magenta and white denote two GNRs and yellow denotes hydrogen bonds. b) A snapshot ($t = 400$ ps) of T-shaped CNT junctions with variable diameters and some defects self-assembled from T-shaped GNRs with rough edges (Figure 5a) at $T = 3\,000$ K.

[1] J. Li, C. Papadopoulos, J. Xu, *Nature* **1999**, *402*, 253.
[2] M. Terrones, H. Terrones, F. Banhart, J. C. Charlier, P. M. Ajayan, *Science* **2000**, *288*, 1226.
[3] D. C. Wei, L. C. Cao, L. Fu, X. L. Li, Y. Wang, G. Yu, Y. Q. Liu, *Adv. Mater.* **2007**, *19*, 386.
[4] J. Park, C. Daraio, S. Jin, P. R. Bandaru, J. Gaillard, A. M. Rao, *Appl. Phys. Lett.* **2006**, *88*, 243113.
[5] P. W. Chiu, M. Kaempgen, S. Roth, *Phys. Rev. Lett.* **2004**, *92*, 246802.
[6] V. Meunier, M. B. Nardelli, J. Bernholc, T. Zacharia, J. C. Charlier, *Appl. Phys. Lett.* **2002**, *81*, 5234.
[7] A. N. Andriotis, M. Menon, D. Srivastava, L. Chernozatonskii, *Phys. Rev. Lett.* **2001**, *8706*, 066802.
[8] M. S. Fuhrer, J. Nygard, L. Shih, M. Forero, Y. G. Yoon, M. S. C. Mazzoni, H. J. Choi, J. Ihm, S. G. Louie, A. Zettl, P. L. McEuen, *Science* **2000**, *288*, 494.
[9] K. S. Novoselov, A. K. Geim, S. V. Morozov, D. Jiang, Y. Zhang, S. V. Dubonos, I. V. Grigorieva, A. A. Firsov, *Science* **2004**, *306*, 666.
[10] J. C. Meyer, A. K. Geim, M. I. Katsnelson, K. S. Novoselov, T. J. Booth, S. Roth, *Nature* **2007**, *446*, 60.
[11] C. Lee, X. D. Wei, J. W. Kysar, J. Hone, *Science* **2008**, *321*, 385.
[12] D. Yu, F. Liu, *Nano Lett.* **2007**, *7*, 3046.
[13] X. L. Li, X. R. Wang, L. Zhang, S. W. Lee, H. J. Dai, *Science* **2008**, *319*, 1229.
[14] L. Tapaszto, G. Dobrik, P. Lambin, L. P. Biro, *Nat. Nanotechnol.* **2008**, *3*, 397.
[15] X. T. Jia, M. Hofmann, V. Meunier, B. G. Sumpter, J. Campos-Delgado, J. M. Romo-Herrera, H. B. Son, Y. P. Hsieh, A. Reina, J. Kong, M. Terrones, M. S. Dresselhaus, *Science* **2009**, *323*, 1701.
[16] P. Koskinen, S. Malola, H. Hakkinen, *Phys. Rev. Lett.* **2008**, *101*, 115502.
[17] D. E. Jiang, B. G. Sumpter, S. Dai, *J. Chem. Phys.* **2007**, *126*, 134701.
[18] A. J. Du, S. C. Smith, G. Q. Lu, *Nano Lett.* **2007**, *7*, 3349.
[19] P. Avouris, J. Appenzeller, R. Martel, S. J. Wind, *Proc. IEEE.* **2003**, *91*, 1772.
[20] R. Martel, V. Derycke, C. Lavoie, J. Appenzeller, K. K. Chan, J. Tersoff, P. Avouris, *Phys. Rev. Lett.* **2001**, *87*, 256805.
[21] P. Avouris, R. Martel, V. Derycke, J. Appenzeller, *J. Phys. B* **2002**, *323*, 6.
[22] J. Q. Lu, J. Wu, W. H. Duan, B. L. Gu, *Appl. Phys. Lett.* **2004**, *84*, 4203.
[23] Y. Huang, X. F. Duan, Y. Cui, L. J. Lauhon, K. H. Kim, C. M. Lieber, *Science* **2001**, *294*, 1313.
[24] P. R. Bandaru, C. Daraio, S. Jin, A. M. Rao, *Nat. Mater.* **2005**, *4*, 663.
[25] H. Q. Xu, *Nat. Mater.* **2005**, *4*, 649.
[26] L. W. Liu, J. H. Fang, L. Lu, F. Zhou, H. F. Yang, A. Z. Jin, C. Z. Gu, *Phys. Rev. B* **2005**, *71*, 155424.
[27] D. V. Kosynkin, A. L. Higginbotham, A. Sinitskii, J. R. Lomeda, A. Dimiev, B. K. Price, J. M. Tour, *Nature* **2009**, *458*, 872.
[28] L. Y. Jiao, L. Zhang, X. R. Wang, G. Diankov, H. J. Dai, *Nature* **2009**, *458*, 877.
[29] M. P. A. a. D. J. Tildesley, *Computer Simulation of Liquids*, Oxford University Press, New York **1987**.
[30] D. W. Brenner, O. A. Shenderova, J. A. Harrison, S. J. Stuart, B. Ni, S. B. Sinnott, *J. Phys.: Condens. Matter* **2002**, *14*, 783.
[31] L. Chico, V. H. Crespi, L. X. Benedict, S. G. Louie, M. L. Cohen, *Phys. Rev. Lett.* **1996**, *76*, 971.

Received: May 29, 2009
Published online: November 19, 2009